Optimizing Processing Time of Radio-Astronomy Antenna Simulations Using FEKO

Rowanne Steiner [1,2], Daniel C. X. Ung [1], Anouk Hubrechsen [2], Robert D. Jones [3], Randall B. Wayth [1], Mark J. Bentum [2], and A. Bart Smolders [2]

[1] International Centre for Radio Astronomy Research, Curtin University, Perth, Australia
[2] Eindhoven University of Technology, Department of Electrical Engineering, Eindhoven, The Netherlands
[3] Colorado School of Mines, Department of Electrical Engineering, Golden, United States of America

Abstract ─ The far-field pattern of a geometrically large and complex antenna used in low-frequency radio astronomy is computationally expensive to simulate on electromagnetic simulators, such as FEKO. For example, one station of the Square Kilometer Array, which consists of 256 log-periodic antenna elements, will take years to simulate using the full CAD model for the full operational frequency band. This paper focuses on reducing the simulation time for a single antenna element by simplifying the simulation model, thus decreasing the number of unknowns that have to be solved in a simulation. An iterative process for optimizing the simplification of such an element is described, while keeping the reflection coefficient within 1 dB absolute mean deviation of the measured data. After four iterations, the amount of unknowns to be solved, which includes the number of triangles and segments, was reduced from 29,307 to 11,991. This decreased the computation time by 86.5%, making array simulations feasible. Using the techniques described in the paper, other antenna constructions can benefit from it and be simulated more efficiently.

Index Terms ─ Antenna, FEKO, optimization techniques, radio astronomy, square-kilometer array

I. INTRODUCTION

The Square Kilometer Array (SKA), a new generation radio telescope, is being used to explore the universe. This array operates in the 50-350 MHz frequency band. The SKA consists of two parts, one in Australia and one in South-Africa. The low-frequency array will be built in Australia and will consist of 512 stations, each of which has 256 pseudo-randomly placed antenna elements. This work is focused on modeling a single element of an individual station, which was deployed at the end of 2019 in the Western Australian desert, see Fig. 1 [1]. The elements of the array are the SKA log-periodic antenna version 4.1 (SKALA-4.1) which was designed by the Italian company Sirio Antenne in CAD [2]. Design fundamentals are presented in [3], [4]. Figure 2 shows the original model of the SKALA-4.1.

Fig. 1. Illustration of the bird's eye view of the SKA array.

FEKO, licensed by Altair Engineering, was used in simulating the antenna [5]. FEKO meshes the antenna using 2D triangles and 1D wire segments, generating unknowns that are solved for using Method of Moments (MoM) [6], [7]. The 2D triangles give rise to more unknowns than the 1D wire segments which increases the processing effort (time and memory wise). To simplify the domain, 1D segments should be used instead of the 2D triangles wherever possible, without sacrificing accuracy of the simulated far-field pattern and scattering parameters (*S*-parameters). The density of the mesh increases when simulating irregular surface features, such as cracks, gaps, and corners. A highly dense mesh is necessary in order to accurately represent these surfaces, but at the expense of an increase in computation time. For this antenna, the focus laid on simplifying or

Submitted On: March 10, 2020
Accepted On: July 5, 2020
https://doi.org/10.47037/2020.ACES.J.351007

eliminating these irregular features to reduce mesh density and speed up performance. Important to note is that for most radio-astronomy applications, most of these intricate structures are small compared to the operational wavelength (< λ/10 [8]). Therefore, they could often be removed or simplified without changing the antenna performance significantly in the operational band [9]-[11].

Simulating the full array is the only way of determining its radiation pattern as it cannot be measured in regular measurement facilities, such as anechoic chambers, due to its size. The original array was computationally expensive, such that it was impossible to simulate with the available amount of RAM (the memory requirement was approximately 420 TB using MoM alone). Even with using the multilevel fast multipole method (MLFMM), which significantly reduces computational time and memory requirements, the memory requirement was still approximately 5 TB for the full array. Due to time and monetary constraints, it was not a viable solution to accept a simulation time of multiple years to cover the entire frequency band, or to make computing-hardware improvements. Instead, processing-time and memory-requirement improvements can be achieved by changing the antenna model in such a way that fewer intricate surface features occur, while still maintaining accuracy. A station consists of 256 antennas, so if the processing time for the model of a single antenna can be reduced, the total array simulation time will drastically improve as well. Therefore, in this work, only the simplification of a single element of the array will be discussed and not the array as a whole. We used MoM to simulate the antenna, since MFLMM does not work for single-element simulations due to the high coupling between the individual mesh. The simplification techniques presented in this paper are applicable for other antenna simulations where either a limited amount of computational resources are available or if the antenna elements are a part of a larger array simulation.

This paper shows an iterative process of modifying the SKALA-4.1 CAD model, without sacrificing important electromagnetic properties, to optimize processing time for numerical electromagnetic modeling. The primary goal of this paper is to present a methodology for optimizing numerical modeling for radio-astronomy or low-frequency antennas. To the authors' best knowledge, such a work does not exist yet in the community. For all iterations, it was critical that there is a near perfect match between the simulations and measurements with the main metric of interest being the reflection coefficient (S_{11}), which is the most sensitive to slight changes. We show far-field patterns as well, but these are not compared with measurement data, as it is not available for this antenna. Section II shows all tips and tricks used for optimizing the SKALA-4.1 model over the course of four iterations. Additional optimization techniques are discussed in Section III and the work is concluded in Section IV.

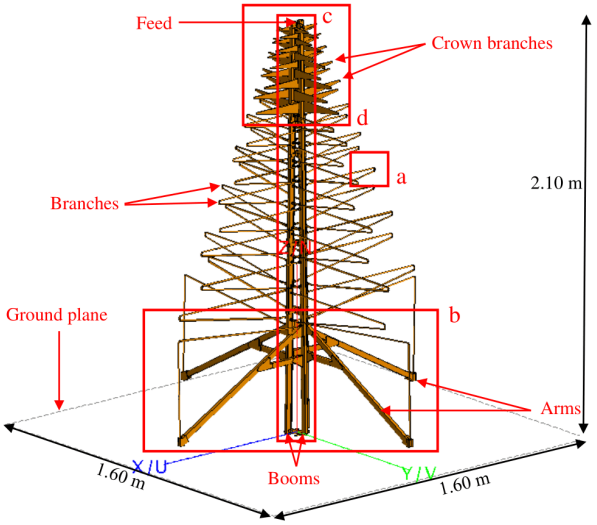

Fig. 2. Iteration-0 of the SKALA-4.1 in FEKO with indicated areas.

II. MODEL: OPTIMIZATION TECHNIQUES AND RESULTS

FEKO simulations were carried out on a dedicated computer system, which has 4 Intel Xeon E5-4640 CPUs containing 8 physical cores each, giving a total 32 processors (multi-threading was disabled as FEKO prefers physical cores over logical cores). It has 128 GB of RAM available. No graphics processing units (GPU) were used [12].

Accuracy is assured by requiring the simulated results to not deviate more than 1 dB on average from measured results over the entire frequency range. The measured results for a single SKALA-4.1 antenna were taken in a semi-anechoic chamber by the National Institute of Astrophysics in Italy (INAF). The 1 dB deviation criteria is calculated by taking the absolute difference between the measured and simulated S_{11} on a logarithmic scale according to:

$$\text{Deviation (dB)} = \left|20\log_{10}(S_{11,\text{simulated}}) - 20\log_{10}(S_{11,\text{measured}})\right|, \quad (1)$$

where we used S_{11} on a linear scale. For accuracy, the main metric is the deviation of S_{11} from the measured data. Far-field patterns are shown as well, both cross- and co-polarization, but it should be noted that those results are less sensitive to model changes compared to S_{11}. Also, no far-field pattern measurement data was available, due to measurement constraints, such as meeting the far-field criterion in a regular anechoic room. Further details of the SKALA-4.1 are presented in [13].

A. Iteration-α: Removing intricate components

The original simulation, iteration-α, was based on the mechanical CAD model of the antenna. This model contained a significant amount of intricate components, such as small screws or non-conducting materials (i.e., plastic) that were not electromagnetically significant (most were << λ/10), but did increase the density of the mesh considerably. The inclusions of the screws used to secure the antenna arms to the boom was unnecessary for electromagnetic modeling and accounted for a couple of thousands in the total mesh count. In the first FEKO computable version, these types of structures were either deleted or replaced.

In MoM wires are meshed with cylindrical segments and in order to be able to simulate these segments, the segment length should be sufficiently large compared to the wire radius [14]. This problem particularly arose in the ends of the branches, see part *a* of Fig. 2, which were round instead of square and thus overly segmented, creating errors in FEKO. Results are described from iteration-0 on, because iteration-α could not even run in FEKO, due to a high computational demand.

B. Iteration-0: The baseline

The first usable model, further referred to as iteration-0, has a run-time of 0.505 hours for a single antenna per frequency. To simulate the entire frequency range of 50-350 MHz with a 1 MHz frequency spacing, it would take more than 6 days to run one single antenna, with an expected duration of multiple years when performing an embedded element simulation.

The amount of unknowns for a single antenna in iteration-0 was 29,307, of which 18,621 were metallic triangles. The absolute mean deviation of the reflection coefficient from the measured data is 0.85 dB. See Fig. 3 for the reflection coefficients of the measured data and all iterations. See Table 1 for a summary of the amount of unknowns, processing time, and time reduction. See Table 2 for the absolute mean difference of the reflection coefficient for all iterations. As mentioned before, the main accuracy metric is the deviation of S_{11} from the measured data. A flowchart visible in Fig. 10 shows a short summary of the main changes in each successive iteration. The ground plane was modeled using an infinite perfect electric conductor in all iterations which is not meshed in FEKO, thus saving computational requirements.

C. Iteration-1: Replacing 3D structures by wires

The focus for the next iteration is on part *b* of Fig. 2, referred to as 'arms', where we change the square tube shape to a wire one, since wires take less processing time compared to other structures. In this iteration, the arms are modeled as wires due to the significant speed improvement over modeling them with plates, see Fig. 4.

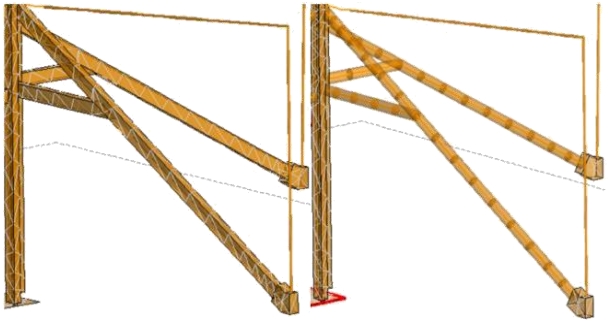

Fig. 4. Square arms of iteration-0 (left), the arms modeled as a wire in iteration-1 (right).

In order to keep the input impedance the same, the cross-sectional area of the arms in square meters is kept equal to iteration-0 according to $l_{\text{tube}} \cdot w_{\text{tube}} = \pi \cdot r_{\text{wire}}^2$, where l_{tube} and w_{tube} are the length and the width of the tube, respectively, and r_{wire} is the radius of the wire, all in meters. Given that l_{tube} = 0.015 m and w_{tube} = 0.025 m, $l_{\text{wire}} \approx$ 0.01093 m was used.

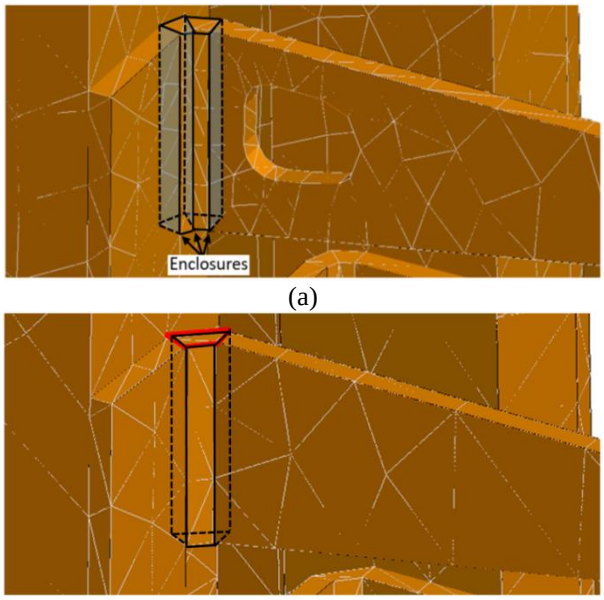

(a)

(b)

Fig. 5. A zoom-in on the change in the top row of crown branches as described in section II D. (a) Top row of crown branches, part *e* of Fig. 2 of iteration-1 including enclosures. (b) Top row of crown branches iteration-2.

These changes caused a reduction in total number of unknowns by 1400 compared to iteration-0. Processing time was also reduced by 23.6%, see Table 1. This process can also be applied for higher frequencies, given that the effective area is kept the same.

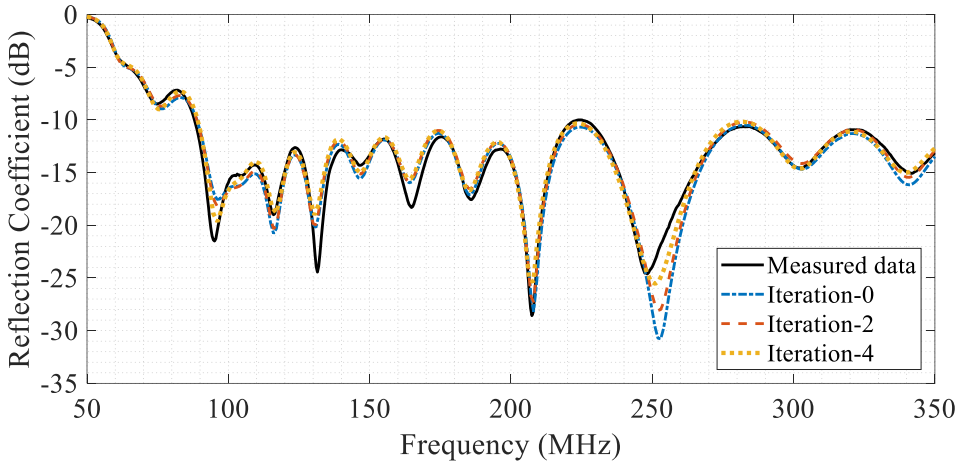

Fig. 3. The SKALA-4.1 (single antenna) reflection coefficient over the frequency range 50 to 350 MHz, for the actual measured data and iteration-0, -2 and -4 in dB.

D. Iteration-2: Simplifying the manufacturing aids

There are four changes in this iteration. First, four holes in the highest row of crown branches were removed, as shown in Fig. 5. The holes are a manufacturing need, but have insignificant effect on the simulated performance, because they are electrically very small. Second, the attachment of the plate onto the boom was simplified from a fillet to a chamfer, as pictured by the red outline Fig. 5 (b), instead of using three smaller structures as shown in Fig. 5 (a). Third, multiple internal plates in the attachments of the crown branches were removed so there are no inside enclosures, see Fig. 5. Three internal plates per crown branch were removed, summing to 120 internal plates for one antenna.

Lastly, the round source feed was replaced by a square one with the same effective area. As mentioned in Section II-A, round structures require a denser mesh compared to square or triangular structures. This geometry change is possible because the round source feed is small compared to the wavelength and will have a small impact on impedance as the same effective area is maintained. These changes resulted in a decrease of more than 9,000 mesh elements compared to iteration-0, and a 63.2% decrease in processing time compared to iteration-0 (see Table 1). The absolute mean difference in S_{11} was 0.72 dB after this iteration (see Table 2).

Table 1: Optimization data for a single polarization for all iterations

Iter.	Nr. of Unknowns	Nr. of Triangles	Nr. of Segments	Processing Time/Freq.	Time Reduction
0	29307	18315	950	0.505	-
1	27953	17665	1038	0.386	23.6%
2	20017	12623	1034	0.186	63.2%
3	18519	11687	938	0.158	68.7%
4	11991	7471	934	0.068	86.5%

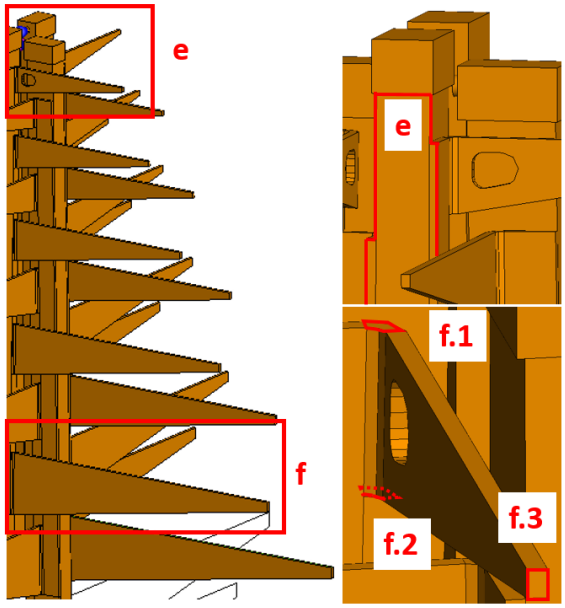

Fig. 6. Part *d* of Fig. 2 of iteration-0 of a single element of the SKALA-4.1 with indicated areas.

E. Iteration-3: Introducing coarse meshing

In order to further reduce the mesh density, the sides of the booms were made into one polygon (red outline in part *e* of Fig. 6). The mesh settings were then set to coarse meshing, an option in FEKO, resulting in a faster simulation due to the mesh being sparser, but with the possibility of being less accurate (especially in small structures). However, due to the relatively large wavelength the meshing could be more coarse here without comprising the accuracy. The resulting amount of unknowns is now around 18,500 and a time reduction of 68.7% compared to iteration-0. The coarse mesh setting is used in all following iterations.

Table 2: Simulated versus measured reflection-coefficient deviation

Iter.	Absolute Mean Difference (dB)	Reduction
0	0.85	-
1	0.84	0.6%
2	0.72	15.1%
3	0.74	12.6%
4	0.60	29.8%

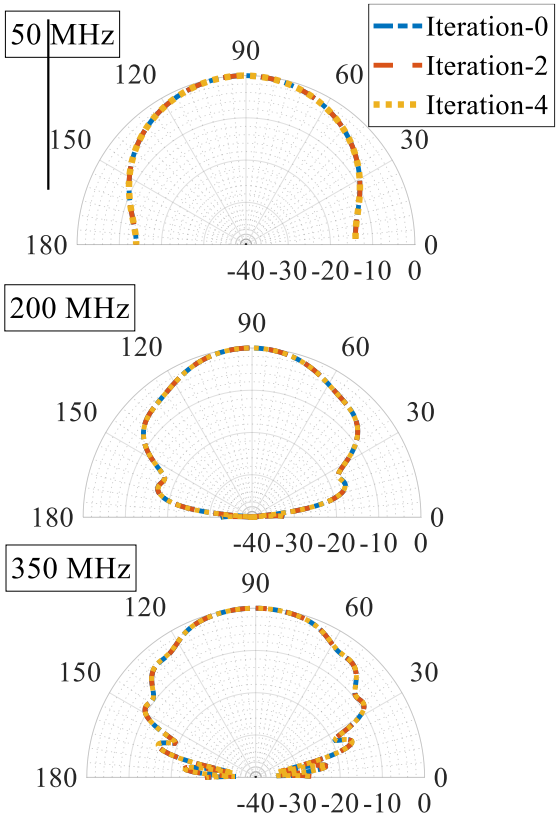

Fig. 7. The normalized co-polarized E-plane radiation patterns of iteration-0, 2 and 4 for the frequencies 50, 200 and 350 MHz (top to bottom) in dB.

F. Iteration-4: Replacing small areas by large surfaces

This iteration focuses on part *f* in Fig. 6. The crown branches were densely meshed, even after the simplification in iteration-2, due to small plates (*f*.1-3 in Fig. 6) that are present at the ends of the branch and at the joints. A single crown branch is hollow and consists of one upper and one lower rectangle to connect them, one top and bottom polygon (red outline at part *f*.1 and *f*.2 of Fig. 6), and one square at the outer end of the crown branch (part *f*.3 in Fig. 6). We removed the polygon on the top of the crown branches (part *f*.1 in Fig. 6) and we removed the square at the end (part *f*.3 in Fig. 6), with an exception for the lowest three crown branches. Removal of *f*.3 in the lowest three crown branches caused a significant effect on S_{11} because the loss in are of *f*.3 is much greater than in the higher crown branches. Loss of a larger area causes a significant difference in the currents flowing through the antenna [15]. The amount of mesh elements went down by about 2,500, with no significant effects on the antenna parameters. The polygon on the top of the lower three rows of crown branches and the bottom polygon of all of the crown branches was removed. This caused the number of unknowns to decrease by another 5,000.

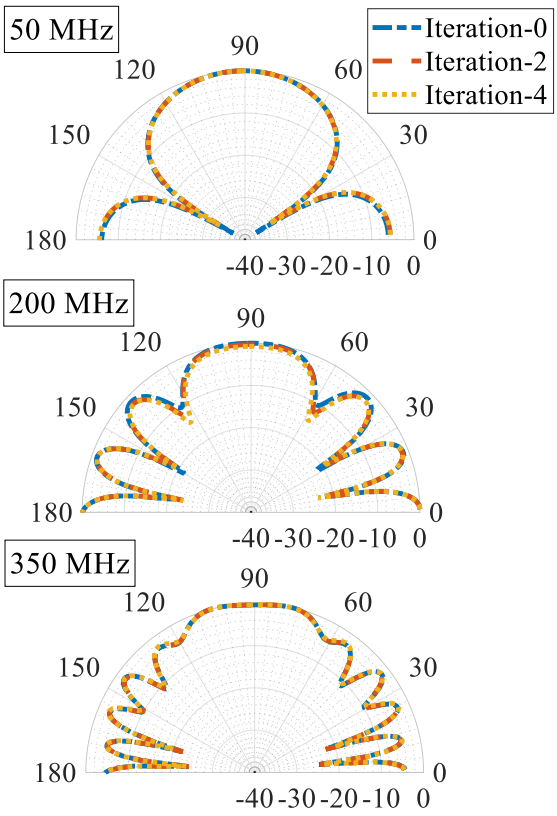

Fig. 8. The normalized cross-polarized E-plane radiation patterns of iteration-0, 2 and 4 for the frequencies 50, 200 and 350 MHz (top to bottom) in dB.

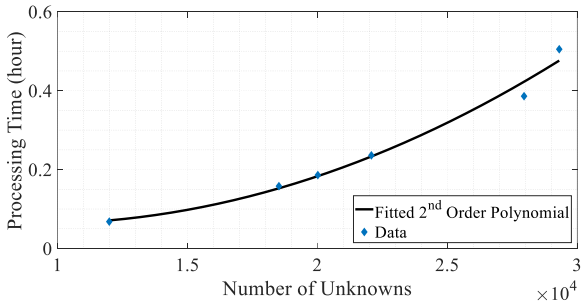

Fig. 9. Processing time per frequency for a single antenna per number of unknowns plotted with a second order polynomial.

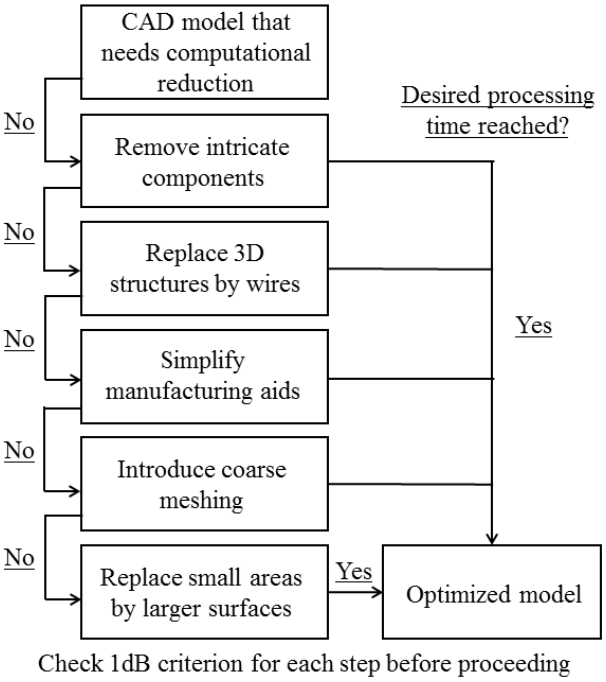

Fig. 10. Flowchart of the proposed approach.

These changes result in a final iteration-4, with about 12,000 mesh elements in total. The absolute mean difference for iteration-4 compared to the measured data in S_{11} is 0.6 dB, which is almost 30 % less deviation from the measured data than iteration-0 (see Table 2). We expect this is caused by the complex structures that occur in the full CAD model, causing higher inaccuracies as compared to measured data. Therefore, simplification can be of advantage in both optimizing processing time and accuracy. A summary of the main optimization techniques used in all iterations is visible in Fig. 10. The co- and cross-polarized E-planes for iteration-0, 2 and 4 are displayed in Fig. 7 and Fig. 8. Figure 9 shows that the computational time for this model indeed expands to the square of the amount of unknowns as expected, as indicated by a second order polynomial fit.

G. Array simulations

After all optimizations, array simulations were made possible again with the amount of available RAM. The single-element modeling of the last iteration for the full frequency range had a processing time of approximately 3 hours. Due to the pseudo-random nature of the array, an array factor can be accurately computed in a matter of seconds and applied to a single element, significantly speeding up the array computation. Note that this approach does not yield accurate results for all radio-astronomy arrays, it highly depends on the array configuration. To verify the use of an array factor, full-wave array simulations were performed as well, which were in good agreement with the array-factor results, but they varied significantly in processing time between the lower and higher-end of the operational frequency band. For lower frequencies, the coupling of the array is significantly higher as compared to higher frequencies, increasing the memory-requirement in the pre-conditioning stage and hence, the processing time [16]-[18]. Therefore, it becomes complicated to extract the processing time for a full-wave array simulation from the processing time of a single element. Note that a significant improvement has been made since the original model did not allow for full array simulations due to a lack of RAM.

III. OVERVIEW AND ADDITIONAL OPTIMIZATION TECHNIQUES

Figure 10 shows a general overview of steps that can be taken to optimize processing time in numerical electromagnetic modeling of radio-astronomy or low-frequency antennas. As this work has shown, optimizing the model can significantly decrease processing time in a low-cost and efficient way, as compared to improving computational hardware. In general, one should always assess important metrics as the reflection coefficient and the far-field patterns for each iterations, such that they do not change significantly in between. It should be noted that most of these optimizations were possible as the structures that were changed were often small compared to the wavelength, or they did not affect the simulated results significantly at low frequencies, such as the coarse meshing option. However, optimizations such as replacing 3D structures with wires are useful at higher frequencies as well.

Additional optimization attempts were made by first changing the main boom (area *c* in Fig. 2) into wires, but this did not satisfy the 1 dB criterion anymore, as the top part of the antenna (part *d* in Fig. 2) consisted of plates which cannot be attached to a wire. Second, an attempt was made to replace the crown branches with wires as well, as these were the greatest source of triangular mesh elements. However, this lead to a significant loss of area for current to flow through, leading to a deviation in S_{11} over 1 dB. This shows the importance of assessing the deviation before applying more simplifications.

IV. CONCLUSION

This work has shown an iterative process for optimizing processing time of the SKALA-4.1, a radio-astronomy antenna. After all iterations, the number of unknowns was brought down from 29,307 to 11,991, which resulted in a reduction in processing time of 86.5%. Using the available hardware, a full-wave array simulation can now be solved in about 7 months instead of an estimated multiple years, and in 3 hours with the use of an array factor. The reflection coefficient of this final iteration represents the measured data 29.8% more accurately compared to iteration-0, and also stays within

the accepted 1 dB deviation from the measured data. In addition to that, the radiation pattern of the latest iteration aligns within 1 dB error with the radiation pattern of the first iteration. A general approach was presented for optimizing processing time for such applications, starting from a CAD model, which can serve as a useful tool for radio-astronomy and low-frequency antenna designers.

ACKNOWLEDGMENTS

The authors would like to thank Pietro Bolli from INAF for providing the CAD model and the measurement data of the reflection coefficient.

REFERENCES

[1] D. Luchetti, 7 January 2020. Australian SKA Project Director's Update. Retrieved from: https://www.industry.gov.au/news-media/square-kilometre-array-project-news/australian-ska-project-directors-update-december-2019

[2] Autodesk, AutoCAD, 2019. [Online]. Available on: https://altairhyperworks.com/product/FEKO/

[3] E. de Lera Acedo, N. Razavi-Ghods, N. Troop, N. Drought, and A. J. Faulkner, "SKALA, a log-periodic array antenna for the SKAlow instrument: Design, simulations, tests and system considerations," *Experimental Astronomy*, vol. 39, no. 3, pp. 567-594, Oct. 2015.

[4] P. E. Dewdney, P. J. Hall, R. T. Schilizzi, and T. J. L. W. Lazio, "The square kilometre array," *Proceedings of the IEEE*, vol. 97, no. 8, pp. 1482-1496, Aug. 2009.

[5] "Altair, FEKO, Suite 2018." [Online]. Available on: www.feko.info

[6] S. Rao, D. Wilton, and A. Glisson, "Electromagnetic scattering by surfaces of arbitrary shape," in *IEEE Transactions on Antennas and Propagation*, vol. 30, no. 3, pp. 409-418, May 1982.

[7] W. C. Gibson, *The Method of Moments in Electromagnetics*. *Chapman Hall/CRC*, London, 2008.

[8] D. Miron, *Small Antenna Design*. Pergamon, London, 2006.

[9] R. F. Harrington, *Field Computation by Moment Methods*. Latest Printing by IEEE Press, 1993.

[10] D. B. Davidson, *Computational Electromagnetics for RF and Microwave Engineering*. 2nd ed., Cambridge, UK, Cambridge University Press, 2011.

[11] P. Yla-Oijala and M. Taskinen, "Calculation of CFIE impedance matrix elements with RWG and n/spl times/RWG functions," in *IEEE Transactions on Antennas and Propagation*, vol. 51, 1837-1846, Aug. 2003.

[12] E. Lezar and U. Jakobus, "GPU-acceleration of the FEKO electromagnetic solution kernel," *2013 International Conference on Electromagnetic in Advanced Applications (ICEAA)*, Torino, pp. 814-817, 2013.

[13] P. Di Ninni, M. Bercigli, P. Bolli, G. Virone, and S. J. Wijnholds, "Mutual coupling analysis for a SKA1-LOW station," in *Proceedings of the 13th European Conference on Antennas and Propagation*, pp. 1-5, Apr. 2019.

[14] Bruce R.EMI/EMC *Computational Modeling Handbook*. Springer Science, 1997.

[15] A. Herczyski, "Bound charges and currents," in *American Journal of Physics 81*, 202, 2013.

[16] K. F. Warnick, R. Maaskant, M. Ivashina, D. B. Davidson, and B. D. Jeffs, *Phased Arrays for Radio Astronomy, Remote Sensing, and Satellite Communications*. Cambride University Press, 2018.

[17] R. Maaskant and E. Woestenburg, "Applying the active antenna impedance to achieve noise match in receiving array antennas," in *Antennas and Propagation Society International Symposium, IEEE*, pp. 5889-5892, June 2007.

[18] D. B. Hayman, A. P. Chippendale, A. W. Hotan, R. D. Shaw, S. G. Hay, T. S. Bird, P. J. Hall, and K. P. Esselle, "Measuring radiotelescope phased array feed noise and sensitivity," in *The 8th European Conference on Antennas and Propagation (EuCAP 2014)*, pp. 3526-3530, Apr. 2014.

Rowanne Steiner received her Bachelor degree in Biomedical Sciences from Radboud University Nijmegen in 2016. After this she completed an Electrical Engineering pre-master in 2017 at Technical University Eindhoven, where she also pursued her master's degree, with the main focus antenna design and electromagnetics. She spend four months doing an internship in ICRAR, Curtin Univeristy at Perth, Australia, and graduated in cooperation with Philips Eindhoven.

Daniel C. X. Ung received the B.Eng. degree in E.C. and M.Phil. degree from Curtin University, Perth, WA, Australia in 2015, and 2020 respectively. He has been a Support Engineer with the International Centre for Radio Astronomy, Curtin University, Bentley, WA, Australia, since 2015. Ung received first place in the FEKO Student Competition hosted by Altair Engineering in 2016. His winning entry, "Embedded Element Pattern Beam Model for Murchison Widefield Array", enabled an accurate and accessible beam pattern of the Murchison

Widefield Array for astronomers. He received a summer studentship at the International Centre for Radio Astronomy Research in 2014.

Anouk Hubrechsen received a B.Sc. and M.Sc. degree in Electrical Engineering at the Eindhoven University at Technology in 2017 and 2019, respectively. She was a Foreign Guest Researcher in 2019 at the National Institute of Standards and Technology (NIST), where she worked on reverberation-chamber metrology. She is currently working as a Ph.D. Researcher on the AMICABLE project, researching interference effects in cable bundles. In 2019 she received the regional and district Zonta Women in Technology awards. She is currently vice-chair of Women in Engineering IEEE Benelux.

Robert D. Jones received dual B.S. degrees in Electrical and Mechanical Engineering from the Colorado School of Mines in 2019, where he is currently pursuing his master's degree. Since 2017, he has been a student Researcher at the National Institute of Standards and Technology (NIST), conducting experiments with loaded reverberation chambers. His current research interests are in computational electromagnetics, antenna design, and loaded reverberation chamber metrology.

Randall Wayth is a Radio Astronomer focused on the design, commissioning and science output of the MWA and SKA-Low radio telescopes. He heads the Astronomical Instrumentation programme within ICRAR.

Mark J. Bentum received his M.Sc. degree in Electrical Engineering (with honors) from the University of Twente, Enschede, The Netherlands, in August 1991. In December 1995 he received the Ph.D. degree for his thesis "Interactive Visualization of Volume Data" also from the University of Twente. From December 1995 to June 1996 he was a Research Assistant at the University of Twente in the field of signal processing for mobile telecommunications and medical data processing. In June 1996 he joined the Netherlands Foundation for Research in Astronomy (ASTRON). He was in various positions at ASTRON. In 2005 he was involved in the eSMA project in Hawaii to correlate the Dutch JCMT mm-telescope with the Submillimeter Array (SMA) of Harvard University. From 2005 to 2008 he was responsible for the construction of the first software radio telescope in the world, LOFAR (Low Frequency Array). In 2008 he became an Associate Professor in the Telecommunication Engineering Group at the University of Twente. From December 2013 till September 2017 he was also the program director of Electrical Engineering at the University of Twente. In 2017 he became a Full Professor in Radio Science at Eindhoven University of Technology. He is now involved with research and education in radio science.

His current research interests are radio astronomy, short-range radio communications, novel receiver technologies (for instance in the field of radio astronomy), channel modeling, interference mitigation, sensor networks and aerospace. He is also Head of the Radio Group at ASTRON. Bentum is the Chair of the IEEE Benelux section, Senior Member of the IEEE and of URSI, initiator and Chair of the IEEE Benelux AES/GRSS chapter, and has acted as a reviewer for various conferences and journals.

Bart Smolders was born in Hilvarenbeek, the Netherlands in 1965. He received his M.Sc. and Ph.D. degree in Electrical Engineering from the Eindhoven University of Technology (TU/e) in 1989 and 1994, respectively. From 1989 to 1991, he worked as an IC Designer at FEL-TNO, The Hague. From 1994 to 1997, he was a Radar System Designer with Thales, the Netherlands. From 1997 to 2000, he was project leader of the Square Kilometer Array (SKA) with the Netherlands Foundation for Research in Astronomy (ASTRON). From 2000 to 2010, he has been with NXP (formerly Philips) Semiconductors, The Netherlands, responsible for the innovation in the RF business line. Since 2010, he is a Full-time Professor at the TU/e in the Electromagnetics Group with special interest in antenna systems and applications. He currently leads several research projects in the area of integrated antenna systems operating at frequencies up to 120 GHz for several application domains, including 5G/6G wireless communication, radar sensors and radio-astronomy. He is Junior-past Chairman of the IEEE Benelux section and Past-Chair of the NERG (Nederlands Radio- en Elektronica Genootschap). He is Board member of the SWAN (Stichting Wetenschappelijke Activiteiten van het Nederlands URSI Committee) and member of the Advisory Board of ASTRON. Next to his research activities, he is the Dean of the Electrical Engineering Department of the TU/e. He has published more than 150 papers.